VYSOKÉ UČENÍ TECHNICKÉ V BRNĚ
BRNO UNIVERSITY OF TECHNOLOGY

FAKULTA STROJNÍHO INŽENÝRSTVÍ
ÚSTAV MATERIÁLOVÝCH VĚD A INŽENÝRSTVÍ

FACULTY OF MECHANICAL ENGINEERING
INSTITUTE OF MATERIALS SCIENCE AND ENGINEERING

BIOCERAMIC MATERIALS FOR ADVANCED MEDICAL APPLICATIONS

BIOKERAMICKÉ MATERIÁLY PRO POKROČILÉ LÉKAŘSKÉ APLIKACE

ZKRÁCENÁ VERZE DOKTORSKÉ PRÁCE
SHORT VERSION OF DOCTORAL THESIS

AUTOR PRÁCE — Ing. LENKA NOVOTNÁ
AUTHOR

VEDOUCÍ PRÁCE — prof. RNDr. JAROSLAV CIHLÁŘ, CSc.
SUPERVISOR

BRNO 2015

KEYWORDS
Bioceramics, scaffold, calcium phosphates, polymer replica technique

KLÍČOVÁ SLOVA
Biokeramické materiály, skafold, kalcium fosfáty, polymerní replikační technika

Disertační práce je uložena na oddělení vědy a výzkumu FSI VUT v Brně,
Technická 2, 616 69 Brno.

ISBN
ISSN

CONTENT

1 INTRODUCTION

Nowadays, many people face problems related to bone disorders. Bone tissue is able to completely regenerate by itself if the damaged part is small enough. If not, it is necessary to help bone restore its damaged part by using bone grafts. The most suitable properties naturally have autografts, i.e. parts of bone harvested from the patient's own body, however there is a lack of available tissue material and the necessity of two surgical procedures causes problems. However, the demand of bone graft is huge - a few million people need a bone graft each year [1]. Hence, a development of a new type of synthetic graft, further referred as scaffold, seems to be a promising way.

The requirements on scaffolds are manifold [2]. The ideal scaffold must be biocompatible (e.g. must not elicit an inflammatory response nor demonstrate immunogenicity or cytotoxicity). It should support tissue formation by three dimensional structures with pores allowing cells to migrate throughout the material and support vascularization of the ingrown tissue. Pores must be interconnected with pore size minimally 100 μm in diameter (ideally about 150 - 500 μm) [3, 4]. Besides macropores, microporosity of the walls (< 100 μm) is desirable because it provides a larger surface area which is significant for protein adsorption, cellular adhesion and proliferation [4]. Scaffolds should be further able to create a stable interface with the host bone without fibrous connective tissue. Its surface texture should promote cell adhesion and adsorption of biological metabolites [5]. In addition, it should support cell differentiation and proliferation [6]. Over a few months' time, the scaffold ought to resorb in the body environment. Resorption kinetics should be equal to the bone repair rate in order to facilitate load transfer to developing bone. The by-products must not be toxic and should be easily eliminated via the respiratory or urinary systems [7]. Mechanical properties must be sufficient and the scaffold must not collapse during handling and in vivo during the normal physical activities. Mechanical properties should be ideally similar to host bone. The optimal Young's modulus of cellular scaffold should be in range 0.1–2 GPa. Compressive strength should be 2 to 20 MPa. Scaffolds should be easily manufactured in desired shapes which would match the defect in the bone. Hence, the intrinsic structure as well as the composition plays critical roles in the success of a scaffold.

2 AIMS OF THE THESIS

This thesis aims to contribute to the search for a suitable bone substitute. The main goal was to prepare porous ceramic materials with sufficient mechanical and biological properties that could potentially serve as substitutes of hard tissues. To solve this goal, research was divided into the following steps:

1) Development of ceramic foams with hierarchical porosity up to pore sizes 1500 μm via replication technique. One approach included composite ceramic scaffolds with enhanced mechanical stability due to strong bioinert core based on alumina and/or zirconia. The second approach was focused on development of fully bioactive ceramic scaffolds based on calcium phosphates.
2) Development of bioactive scaffolds by burning out the organic compounds from in situ blown polyurethane / calcium phosphate composite.
3) Study of mechanical and biological properties of the prepared scaffolds.

3 EXPERIMENTAL

MATERIALS

Commercial reticulated polymer foams Bulpren (Eurofoam, Czech Republic) of five different pore sizes (30 to 90 ppi, pores ner inch) were replicated.

Three different oxides: white fused corundum F1200 (Koltex, Czech Republic), synthetic alumina RC HPDBM (Malakoff Ind., US), Yttria stabilized zirconia HWY5.5 SD (Guang Dong Huawang Materials, China) and two calcium phosphate commercial powders hydroxyapatite and beta–tricalcium phosphate (both Fluka, Switzerland) were used. Powders were bonded by polymeric binders (PVA – Mowiol or PVB – Butvar) or by colloidal solutions (1) AlOOH sol Disperal P3 no.10090 (Condea Chemie GmbH, Germany) or (2) colloidal silica Ludox SK-R (Grace, U.S.). Besides powders and binders, other additives such as plasticizers (Glycerol (Onex, Czech Republic), deflocculate (Dolapix CE64 (Zschimmer Schwarz, Germany) or defoaming (n-Octanol ($C_8H_{18}O$, Lachema, Czech Republic) agents were added to prepare stable suspensions.

Diisocyanate Ongronat® 2500 MDI (BorsodChem Zrt., Hungary) and polyol Stepanpol PS-2412 (Stepan Company, US) were used for in situ blown polyurethane /calcium phosphate composites.

METHODOLOGY

Powders, suspensions and sintered scaffolds were characterised by following methods: *Specific surface area* was evaluated via nitrogen adsorption by ChemBET 3000 (Quantachrome, USA) device. *Particle size distribution* by laser diffraction on LA 950 (HORIBA, Japan) device. *Thermal analysis*, was performed by 6300 Seiko Instruments TG-DTA in argon or air/argon (1:1) mixture, flow rate 400 ml / min, ↑2 °C/min. *Zeta potential* was measured in aqueous dispersions by using Zetasizer 3000 HS (Malvern Instruments, UK). *Viscosity* of the prepared sols and slurries was measured using a rotary rheometer Mars II Haake (Thermo Scientific, US). *Phase composition* was determined by X-ray diffractometers SmartLab 3kW (Rigaku, Japan) and PANalytical X'pert (Philips, Netherlands). The *morphology* was observed using scanning electron microscopy (ZEISS Ultra Plus, Germany, Tescan VEGA TS5136XM, Czech Republic and Philips XL30, Netherlands).

Total porosity of scaffolds was calculated as follows [8]: $P = \frac{\rho_t - \rho_b}{\rho_t} \times 100\%$, where ρ_t is the theoretical density and $\rho_b = \frac{m_b}{V_b}$ is the bulk density, m_b is the mass of the dry test piece and V_b is the total geometrical volume. The bulk density of struts was determined via Archimedes'principle (EN 623-2) with distilled water [8]. Image analysis was performed to determine the porosity of struts, the total porosity and pore (cell) sizes and their distribution. The true 3D mean pore diameter was from 2D values recalculated by simple stereological correction factor 0.785 [9].

Mechanical properties of prepared foams were determined using a compression test by high-precision Electric Actuator Systems 8862 (Instron, US) equipped with 5 kN load cell. The crosshead speed of 0.5 mm/min was used for loading in all tests. The compressive strength was determined from the maximal obtained force.

Bioactivity was tested in SBF solution according to Kokubo recipe [10]. *Cytotoxicity* of materials was tested *in vitro* using direct contact assay according to EN ISO 10993-5 specifications [11] with cells of cell line MG-63 (3500 cells/cm^2). *Cell viability* was tested with

adipose-derived stem cells which were isolated from adipose tissue by centrifugation and collagenase extraction, as described in [12]. Cells were trypsinized and seeded on materials at concentration of 50.000/100 µl for analysis cell viability and 1 million cells/100 µl for evaluation of cell morphology. Samples were taken for analysis after 24 hours of cultivation. Cell viability was assessed by live/dead assay. Cells cultivated for 24 hours on all materials were fixed and permeabilized. Actin cytoskeleton was stained with Phalloidin Rhodamine (R415, Lifetech, Czech Republic) dissolved in PBS and cell nuclei were stained with 4',6-diamidino-2-phenylindole (DAPI). Samples were observed with epifluorescence microscope Cell^R (Olympus C&S Ltd., Czech Republic).

CERAMIC FOAM PROCESSING: Ceramic scaffolds were prepared by two techniques: by polymer replica technique and by burning out polyurethane from CaP / PU composites blown in situ from MDI and polyol. By means of replica technique, scaffolds were prepared according to scheme in Fig. 1

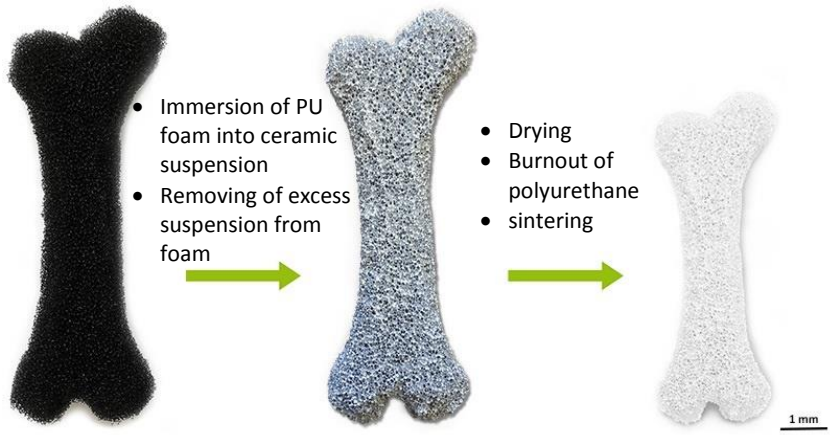

Fig. 1 A scheme of preparation of ceramic scaffold by replication technique: (a) PU template, (b) template coated by suspension, (c) sintered ceramic body

Chemical composition of suspensions, heat treatment and other parameters are described in more detail below.

Alumina based scaffolds: 6 wt.% boehmite sol was after 24 h of aging filled with fused alumina powder (71 to 73 wt. %). The PU foam of initial porosity 30 ppi was used as template to replicate. After heat treatment (800°C / 2h, ↑1 °C/min and 1600 °C /2 h, ↑5 °C/min), the struts were soaked in 8 wt= Dispersal sol for 24 h, 48 h, 168 h and 5×5 h, or were coated by suspension composed of Disperal sol filled with synthetic alumina. Scaffolds after the second sintering (1600 °C /2 h) were coated by hydroxyapatite suspension ball milled in 2% solution of Butvar in IPrOH. The polymer was burnt at 800 °C/2 h and composite sintered at 1250 °C/2h in air atmosphere.

Alumina toughened zirconia based scaffolds: Disperal sol was stabilised to pH 4.0 and after 24 h of aging was filled by zirconia powder. The concentration ratio between boehmite sol and zirconia was calculated for alumina concentration (2.5, 5, 10 wt.%) in composite after sintering. Suspensions contained from 50 to 60 wt. % of solid phase. To achieve different porosities, various number of layers was applied on PU template (45, 60 ppi). The coating and drying procedure was repeated until the desired number of layers was reached (up to 6). Foams sintered at 1550 °C for 2 h in air were coated by suspension containing hydroxyapatite

or beta–calcium phosphate and 2wt. % of Butvar. Composites were sintered at 1200 °C/3h in air.

Calcium phosphate based scaffolds: suspensions were prepared from polyvinylalcohol Mowiol 10-98 (5 wt. %) dissolved in water, 0.05 wt. % octanol, 0.3 wt. % glycerol and at 800 °C calcined hydroxyapatite powder (40 to 50 wt. %.). PU templates of 45, 60, 75 and 90 ppi were burnt out at 1000 °C/ 2 h with heating rate 0.5 °C/min, scaffold was finally sintered at 1200 °C in air.

Calcium phosphate based scaffolds reinforced by silica: hydroxyapatite was bonded by colloidal silica solution Ludox. 5, 10, 15 and 20 wt. % concentration of silica were tested. Powder was added into the water and Ludox mixture. The resulting suspension was agitated by 3D motion generated by Turbula device (Willy A. Bachofen AG, Switzerland) at 98 rpm for 2 h. Suspension was applied on PU templates of porosities of 60, 75 and 90 ppi. Foams were after drying heat treated at 1000°C / 2h and sintered at 1200 or 1250 °C.

Calcium phosphate scaffolds prepared from rigid polyurethane foam: Cellular polyurethane / CaP composite scaffolds were blown by the reaction between the polyisocyanate ONGRONAT 2500, the polyol STEPANPOL PS-2412, deionized water and hydroxyapatite powder. The effect of mixture loading (CaP / PU ratio of 0.4–1.2), added water (0–5 pphp, parts per hundred parts of polyol) and isocyanate index (0.75 to 1.25, preferably set to 1.05) was evaluated. Composite scaffolds were prepared in two steps: (1) polyol, water and powder were mixed, (2) the isocyanate was added afterwards. The resulting mixture was immediately put into a mould and left there for 24 hours to allow the formation and growth of the composite foam. The scaffolds were shaped after 24 h hardening. The organic contents were burnt out in air at 800 °C for 2 hours (or 1050 °C/2 h) with 0.5 °C/min heating rate. Sintering was conducted at 1050 °C/2 h, 1200 °C/2 h and 1350 °C/2 h in air atmosphere.

4 RESULTS AND DISCUSSION

4.1 Bioactive ceramics based on alumina core

Characterization of suspensions

The rheological behaviour of sols and suspensions was studied in order to find suspension with optimal adhesion to PU template, optimum stability and high cover efficiency. Fig. 2a illustrates how time of aging influenced viscosity. The viscosity decreased with increasing time of aging. The shear thinning behaviour occurred in lower shear stresses in the case of shorter aging time (2 and 4 h). The optimal aging time was determined to 24 h, when the supposed de-agglomeration of powder was finished and sol was stabilised with almost Newtonian rheological behaviour.

As shown in Fig. 2, the suspensions with various alumina content (from 71 to 73 wt. %) exhibited shear-thinning behaviour in accordance with published works [13, 14]; viscosity increased with increasing alumina content. Suspension with 72.5 wt. % of alumina revealed an optimal adhesion to PU foam with low degree of sealed struts of foam.

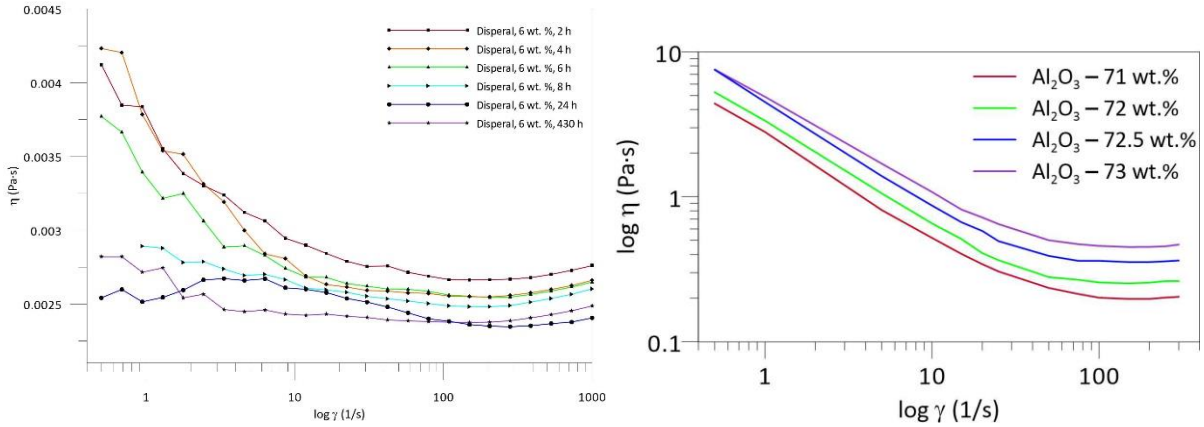

Fig. 2 Rheological behaviour of (a) 6 wt. % dispersal sol, (b) alumina suspensions

Foam morphology

The macrostructure morphology of prepared foams after taking into account the shrinkage was almost the same as one of PU template that was replicated. As is evident from Fig. 3 prepared foams were highly porous without sealed walls of scaffold cells (pores). The average scaffold cell size was 3539 ± 218 µm. The average size of pores that connected cells, sometimes referred as “cell windows” was about 1200 µm. Thickness of hollow struts varied between 260 and 370 µm. The triangular void in the centre of strut (see Fig. 4a) was a main drawback of replica method, because it negatively influenced the mechanical properties of the foam [15]. The total porosity of prepared samples achieved 95%, the porosity of material of struts was almost 50%. This porosity slightly decreased with increasing alumina content. Results indicate that long soaking time had a positive influence on density of strut material.

Fig. 3 Macrostructure of alumina foam (A7250)

Influence of infiltration of Disperal sol on struts morphology is illustrated in Fig. 4. It is evident that the hollow voids inside the struts were not completely filled with nanosized alumina (Fig. 4b), On the contrary, the strut was completely filled by second approach, by coating by microsized synthetized alumina (Fig. 4c)

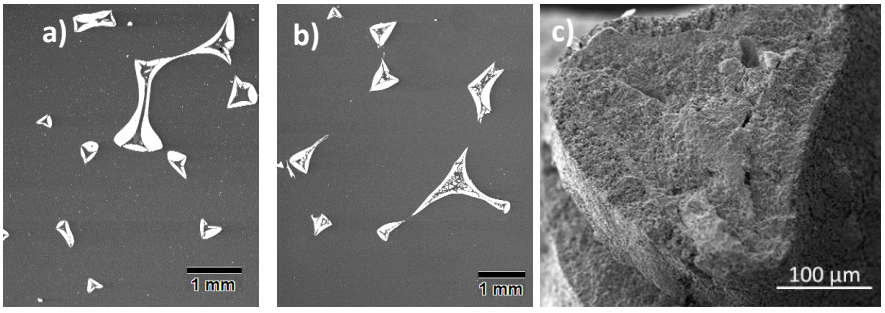

Fig. 4 Cross-section of alumina core: (a) after sintering, (b) after soaking in Disperal sol for 5 × 5– newly formed small alumina particles are visible in pores, (c) Detail of core strut filled by synthetic alumina

This alumina / alumina scaffold was coated by hydroxyapatite suspension to improve biological properties. Fig. 5. shows the layers are strongly bound to each other. The thickness of each layer (synthetized alumina and hydroxyapatite) was about 20 µm.

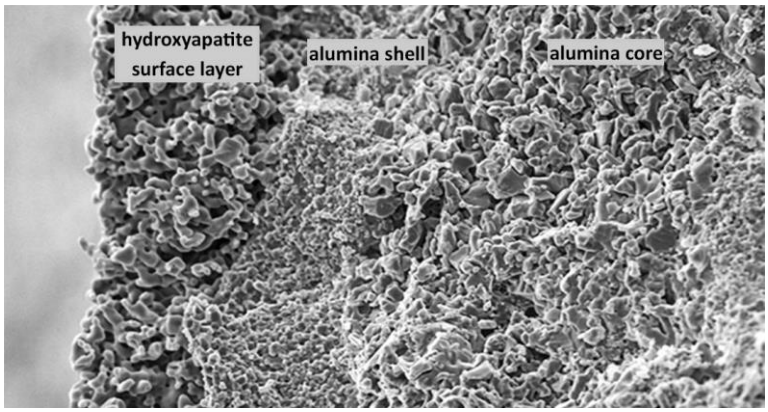

Fig. 5 Microstructure of composite (from right to left: alumina core, alumina shell and hydroxyapatite layer)

Bioactivity

After 14 days of soaking in SBF, the surface of the scaffold was partially covered by newly formed apatite layer in typical cauliflower morphology consisted of thin lamellae as is illustrated in Fig. 6. The formation of bone-like apatite on the surface of alumina / alumina / hydroxyapatite scaffold indicates bioactive behaviour.

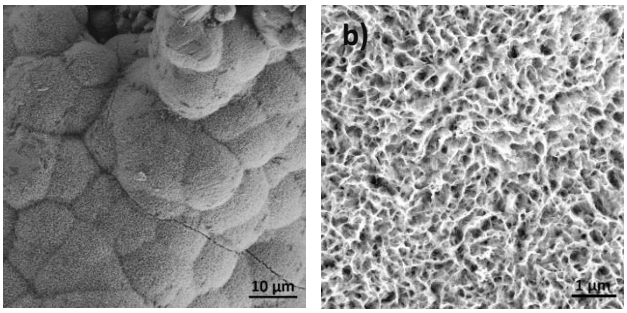

Fig. 6 Surface of alumina / alumina / hydroxyapatite scaffold after 14 days immersion in SBF: (a) typical cauliflower like structure of newly formed apatite; (b) detail of thin lamellae.

Mechanical properties

The overview of the compressive strength values depended on concentration of alumina in suspension and time of soaking by Disperal sol is plotted in Fig. 7.

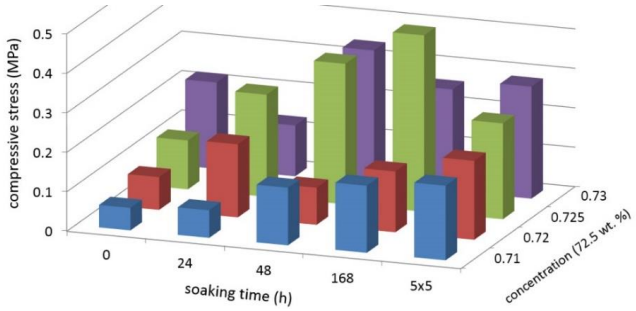

Fig. 7 Compressive strength of alumina foams reinforced by boehmite sol in dependence of various soaking times.

As evident, the short soaking time and/or suspensions with low powder content exhibited low compressive strength due to non-homogenous and insufficient infiltration of the core layer. The optimal processing conditions were powder content of 72.5 wt. % and the soaking time 168 h or 5 × 5 h. Due to high porosity, compressive strength values seemed to be low. By second alumina coating, the porosity of specimens was reduced (mainly due to strut filling) and because strength is exponentially proportional to the porosity, the mechanical stability of the prepared foams was improved (from 0.3 MPa up to 1.2 MPa) as is displayed in Fig. 8.

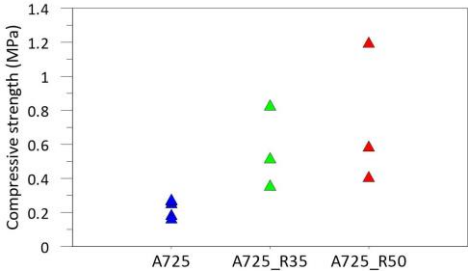

Fig. 8 Compressive strength core-shell alumina composites. A725 – alumina core; A725_R35 – alumina core / alumina shell (35 wt. %); A725_R50 – alumina core / alumina shell (50 wt. %);

4.2 Bioactive ceramics based on alumina toughened zirconia

Bioactive ceramics described in this chapter were composed of zirconia inorganically bonded by boehmite (AlOOH). The amount of alumina in the structure was 2.5, 5 and 10 wt. %. The alumina was added to zirconia because it was reported that it prevents zirconia from unfavourable low temperature degradation in body environment [16]. The amount of alumina produced from decomposition of commercial boehmite was determined via thermal analysis. The total weight loss was 30.5.

Characterisation of suspensions - zeta potential

Zeta potential, a key indicator of the stability of colloidal dispersions was measured in aqueous dispersion of Disperal P3. Colloids with low absolute value of zeta potential (-30 mV to +30 mV) are not efficiently electrically stabilized and tend to coagulate. As is evident from Fig. 9, the dispersions in acidic range behave stably, the highest ζ-potential equalled to +60 mV was measured at pH 4, and therefore the pH of prepared sols was adjusted by acetic acid to this value in the following experiments.

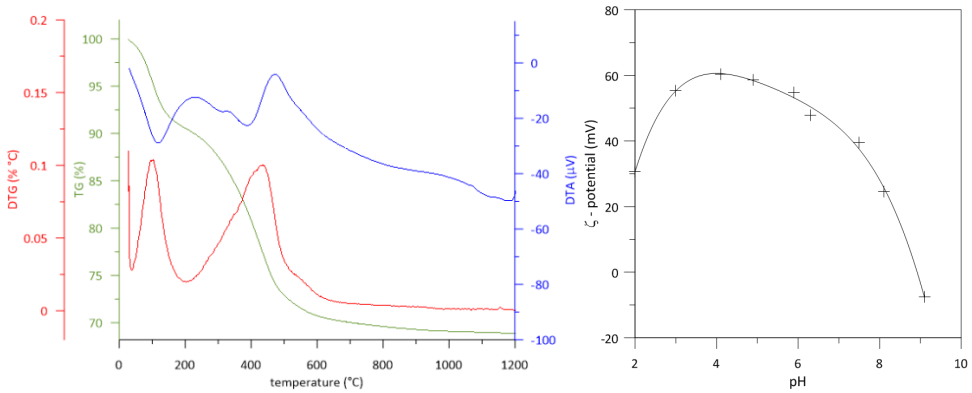

Fig. 9 Left: Thermal analysis of commercial boehmite sol Disperal P3; right: ζ-potential as a function of pH for the dispersion Disperal P3.

Characterisation of suspensions - rheological properties

Suspensions were prepared from 24 h aged boehmite sol which rheological properties were described in previous chapter. From a technological point of view, the optimum suspension for coating the scaffold of 45 ppi contained 60 wt. % of solid phase. However, this suspension was too viscous for coating of scaffolds with smaller pores. To avoid undesirable blocking of open scaffold cells (“macropores”), the scaffolds with 60 ppi and 75 ppi porosity were coated by suspension containing 50 wt. % of solid phase.

Morphology of sintered scaffolds

Scaffolds of total porosity (57–98%) were prepared by multiple coating process (up to 6 repeating). Pore sizes of interconnected macroporous scaffolds varied from 350 to 1200 µm. Scaffold cell size corresponded to the cell size of polyurethane foam reduced by shrinkage. With an increasing number of layers, the average thickness of struts grew from 73 µm to 395 nm. The typical reticulated morphology was lost as porosity decreased below 70 % (in the case of larger pores – 45 ppi) and below 80% (for 60 ppi). Overview of macrostructures of prepared scaffolds is shown in the Fig. 10.

	1 layer	2 layers	3 layers	4 layers	5 layers	6 layers
45 ppi	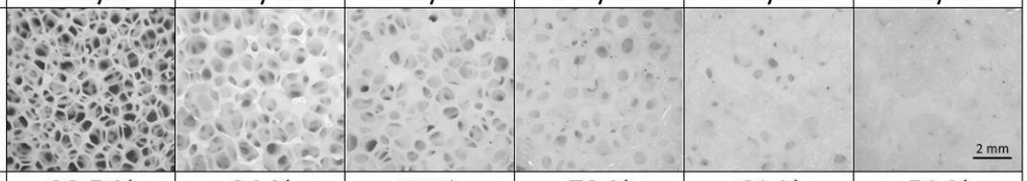					
Porosity:	98.5 %	94 %	88 %	72 %	61 %	51 %
	1 layer	2 layers	3 layers	4 layers		
60 ppi	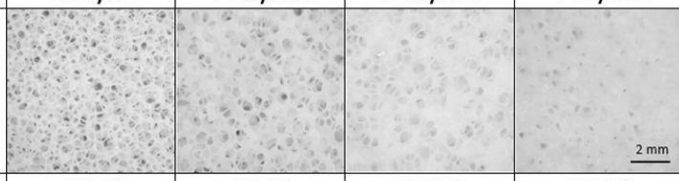					
Porosity:	97 %	91 %	77 %	60 %		

Fig. 10 Dependence of porosity on the number of layers.

Alumina toughened zirconia substrates with desirable porosity were coated by calcium phosphates suspensions in order to improve the biological properties of scaffolds. Scaffolds consisted of 2 layers of ATZ (5% Al_2O_3) and CaP coating are shown in Fig. 11. The thickness of bioactive layer achieved 20 to 60 µm. The struts of ATZ cores were not filled by HA due to closed porosity.

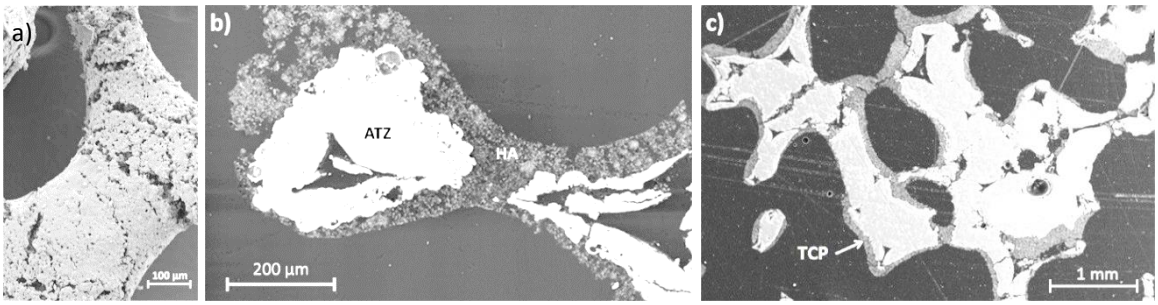

Fig. 11 Structure of the bioactive coatings: (a) a strut with HA coating; (b) cross section of ATZ scaffold coated by HA; (c) cross section of ATZ scaffold coated by β-TCP.

Mechanical properties

The overview of compressive strength values of ATZ scaffolds containing 2.5 to 10 wt. % of alumina is plotted in Fig. 12. It was confirmed that strength decreases with increasing porosity. Material containing 5 % of alumina exhibited highest strength, so this composition was chosen for subsequent biological testing. All tested samples exhibited strength above 0.2 MPa, the minimal value reported for highly porous cancellous bone [17]. Scaffolds for potential applications in bone tissue engineering should have higher density than at least 2 MPa to ensure sufficient strength to withstand forces generated in the body.

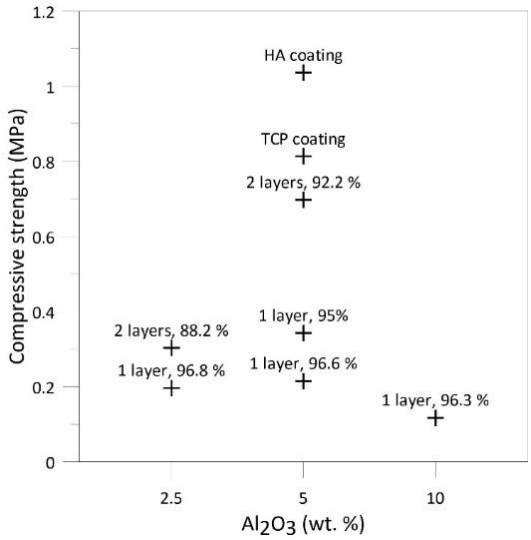

Fig. 12 Compressive strength of ATZ scaffolds

Biological properties – incubation in simulated body fluid

After 28 days of incubation in simulated SBF the surface was completely covered by a self-grown apatite layer. The top view of ATZ substrate and Ca-phosphates coatings before and after 28 days of soaking in SBF is reported in Fig. 13. No change was observed on uncoated ATZ samples.

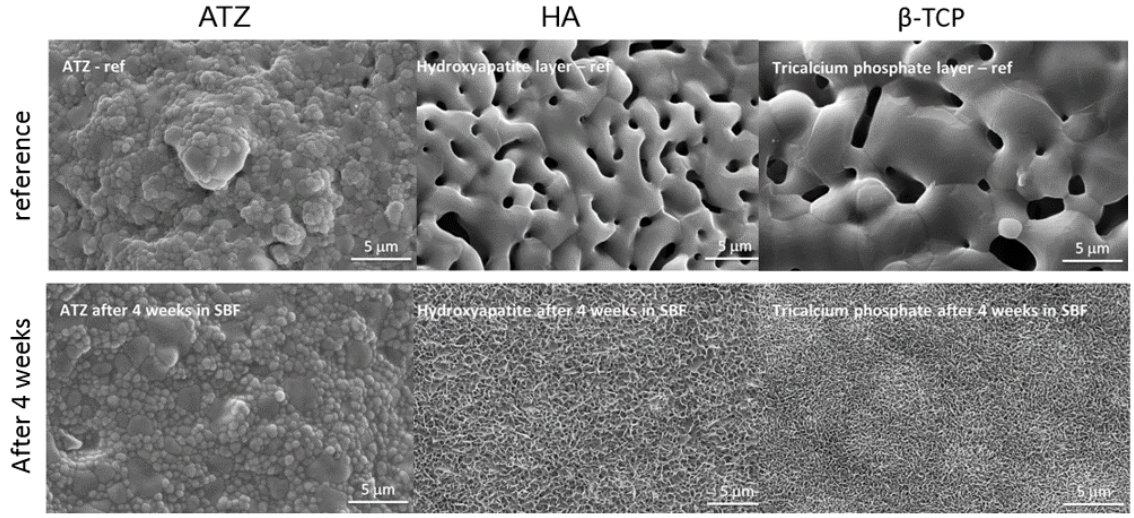

Fig. 13 Microstructure of the substrates and coatings before and after soaking in SBF.

Cytotoxicity evaluation

Although both zirconia and alumina are consider being bioinert in contact with host tissue, the cytotoxicity of the composite was for sure evaluated by direct contact assay. Direct contact between MG-63 cells and all tested materials did not induce any adverse effect, cells retained characteristic morphology of MG-63 cells (see Fig. 14.). SEM was used to study the adhesion and spreading of MG63 cells on the ATZ / Ca-P 3D scaffolds. Micrographs revealed that cells were attached to the pore walls both inside (Fig. 14a) and outside (Fig. 14b) of the 3D structure. These results indicates that cells were able to migrate through 3D structure of composite having the 1200 µm large pores.

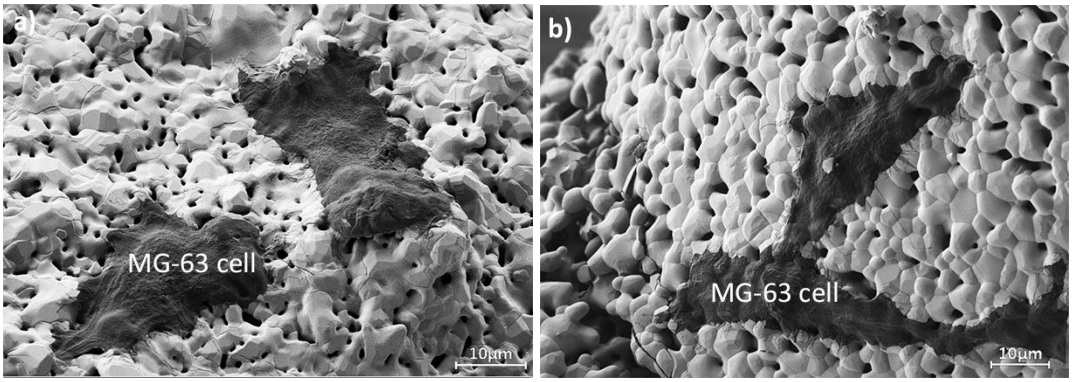

Fig. 14 Cell line MG-63 adhered to the scaffold: (a) on inner struts; (b) on outer struts.

This result confirmed that all tested materials (ATZ, HA, β-TCP) were cytocompatible and could be used in tissue engineering applications.

4.3 Calcium phosphate scaffolds

Several types of polymer binders were tested in order to achieve a reticulated calcium phosphate foams. However prepared scaffolds had mostly insufficient strength due to high porosity (> 90%). Scaffolds prepared from alcohol suspensions had many defects in the structure, probably as a consequence of fast evaporation of alcohol. The best scaffolds were obtain with water suspension bonded by 5 wt. % of PVA. These results are summarized and compared with silica reinforced scaffolds in the Chapter 4.4.

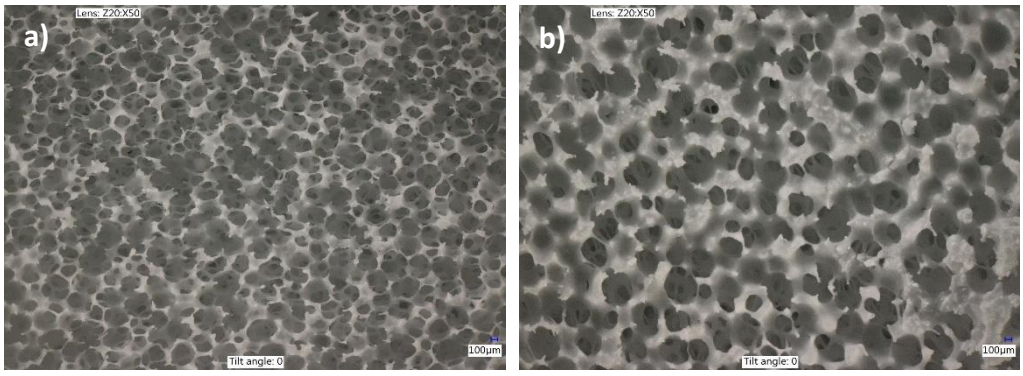

Fig. 15 Structure of calcium phosphate scaffolds sintered at 1200 °C/3 h: (a) template 90 ppi, (b) template 75 ppi

4.4 Calcium phosphate scaffolds reinforced by silica

The objective of this chapter was to develop a material with higher strength and at least similar biological characteristics as hydroxyapatite. The idea was to prepare ceramic composite material containing calcium phosphate with some reinforcing phase. The choice fell on silica because silicon (as Si^{4+} ion) is consider to be one of the essential trace elements required for development of healthy bones. It acts as a biological cross-linking agent in extracellular matrix (ECM). On top of that, it enhances osteoblast proliferation, differentiation and collagen production [18].

Characterisation of scaffolds – processing parameters

Since polymer replica technique was used, ceramic foams were obtained by burning the polyurethane templates. The thermal analysis was carried out to determine the temperature

at which the complete burnout of the commercial polyurethane occurred in the composite system containing PU (10 wt. %), HA (81 wt. %) and SiO_2 (9 wt. %). According to thermogram which is depicted in Fig. 16 all polyurethane was burned at 550 °C. The shape of exothermic DTA curve in the temperature range 200 to 550 °C indicates that the degradation processes of polyurethane occur by oxidation mechanism.

The total 15% weight loss corresponded to the initial amount of polyurethane in the composite (10 %), amount of adsorbed water (1 %) and to 5% weight loss of commercial hydroxyapatite after its calcination (4 % relative to the composite).

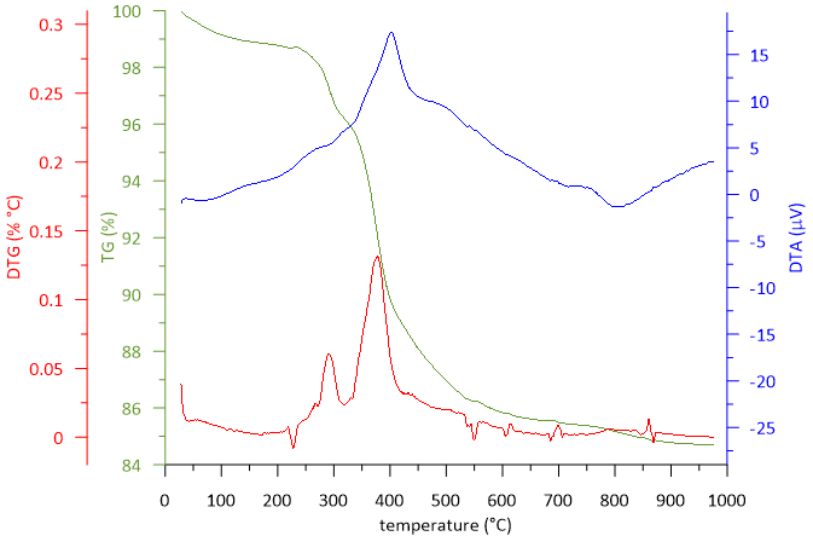

Fig. 16 TA curves of commercial reticulated PU foam coated by HA-10SiO_2 suspension

Phase composition

X-ray diffraction patterns indicated that all products of thermal reaction were crystalline. The XRD spectra illustrated that the hydroxyapatite was totally decomposed into α and β–TCP even at 1200 °C. Traces of tetracalcium phosphate identified in the structure were a result of HA decomposition, according to the following equation [19, 20]:

$$Ca_{10}(PO_4)_6(OH)_2 \xrightarrow{-H_2O} Ca_{10}(PO_4)_6O \rightarrow 2Ca_3(PO_4)_2 + Ca_4(PO_4)_2O \quad (7)$$

If the concentration of silica in the tested sample was low (5 wt. %), walstromite ($CaSiO_3$), an isomorph of wollastonite, was distinguishable in the pattern. With increasing concentration of silica in the sample, one strong peak at about 21.7° increased. That suggests that silica was transformed to the cristobalite crystalline phase (of $P4_12_12$ space group). An approximate weight percentage of phases is listed in Table 1.

Table 1 Phases present in the scaffolds after heat treatment at 1200 °C (HA) and 1250 °C (HA-SiO_2)

	α–TCP (wt. %)	β–TCP (wt. %)	Cristobalite (wt. %)	Other phases (wt. %) / type	α : β–TCP
HA	50.6	49.4	–	–	1.02
HA_5% SiO_2	60.8	34	2.3	2.9 (walstronite)	1.79
HA_10% SiO_2	62	25.3	12.7	–	2.45
HA_15 % SiO_2	59.3	21.1	17.4	2.2 ($Ca_4(PO_4)_2O$)	2.81
HA_20 % SiO_2	65.2	12.5	20.3	2 ($Ca_4(PO_4)_2O$)	5.22

Results indicated that the ratio between α–TCP and β–TCP increased with increasing amount of silica. Various researchers [21-24] confirmed that addition of silica shifted the

temperature of HA→ α–TCP transformation to lower value. The stable α–TCP polymorph could be even formed during sintering above 700 °C [22, 23, 25, 26] [21]. It was further reported that hydroxyapatite sintered in the presence of silica tended to transform to silica substituted tricalcium phosphate (Si–α–TCP) of formula $Ca_3(P_{1-x}Si_xO_{4-x/2})_2$ [21, 26].

Characterisation of scaffold cell size and its distribution

Fig. 17 and Fig. 18 give an overview of scaffolds with various cell size. Structure of HA scaffold and HA–SiO_2 scaffold was very similar. As obvious from Table 2, pores (defined by cell size) were slightly larger in case of hydroxyapatite.

Table 2 Pore sizes of HA-SiO_2 and HA

	Cell size (μm)	Size of cell windows (μm)
HA 60ppi	873 ± 55	262 ± 80
HA 75ppi	532 ± 67	204 ± 78
HA 90ppi	385 ± 60	116 ± 45
HA-SiO_2 45ppi	1150 ± 198	536 ± 113
HA-SiO_2 60ppi	736 ± 85	287 ± 92
HA-SiO_2 75ppi	498 ± 58	168 ± 45
HA-SiO_2 90ppi	375 ± 37	118 ± 35

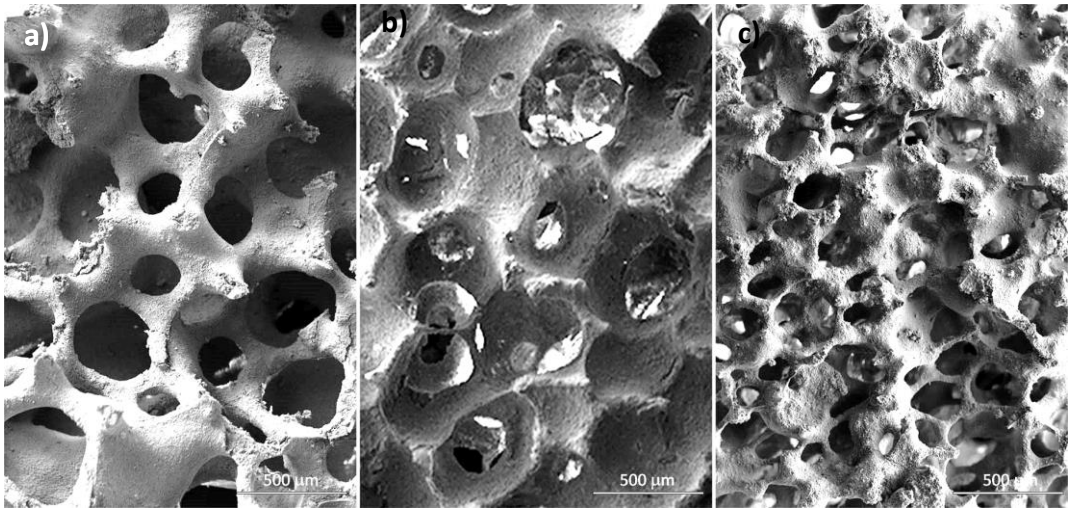

Fig. 17 HA scaffolds sintered at 1200 °C/3h; porosity of the PU template: (a) 60 ppi, (b) 75 ppi, (c) 90 ppi

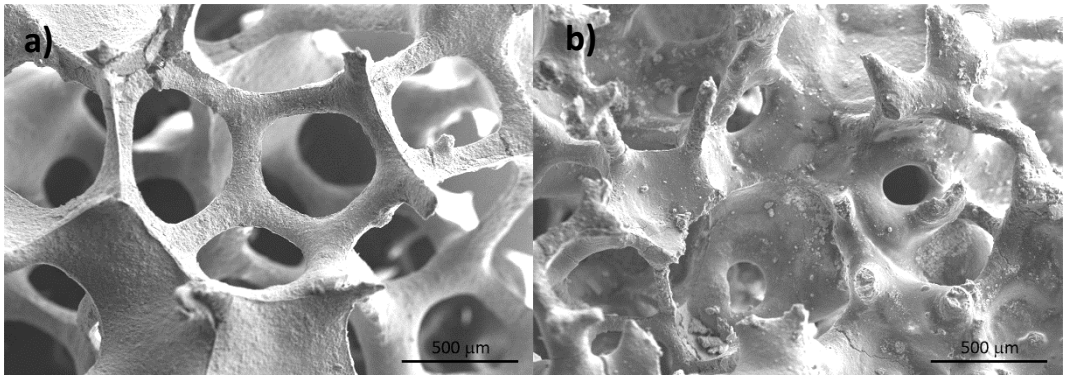

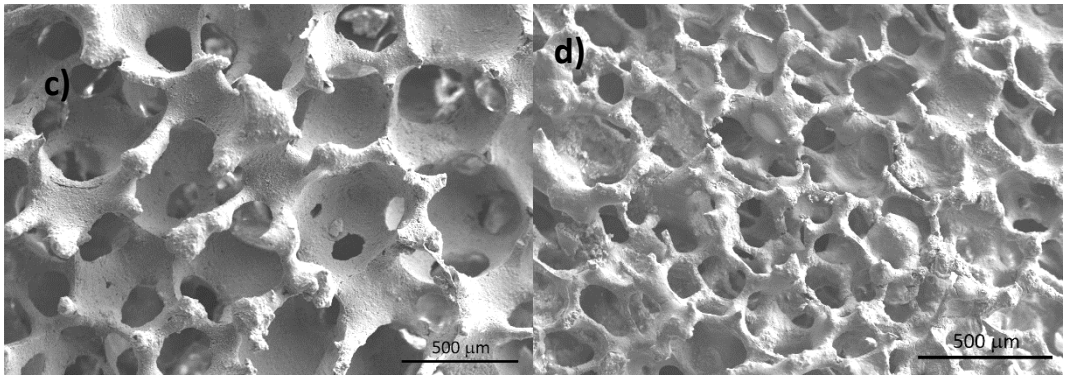

Fig. 18 HA-10SiO_2 scaffolds sintered at 1250 °C/3h; porosity of the PU template: (a) 45 ppi, (b) 60 ppi, (c) 75 ppi, (d) 90 ppi

Biological properties - bioactivity

Bioactivity of prepared scaffolds was tested in Eagle medium instead of in simulated body fluid Fig. 19 presents the overview of surface morphology of prepared scaffolds before and after immersion in medium. After 3day cultivation in direct contact assay, the surface of scaffolds was covered by newly formed apatite layer. Samples containing silica were fully covered whereas layer of apatite precipitated on pure CaP were not continuos. It could have been caused by high porosity of the sample. Newly formed apatite layer, nucleated under the conditions simulated in vivo indicates a good bioactivity of scaffolds containing cristobalite.

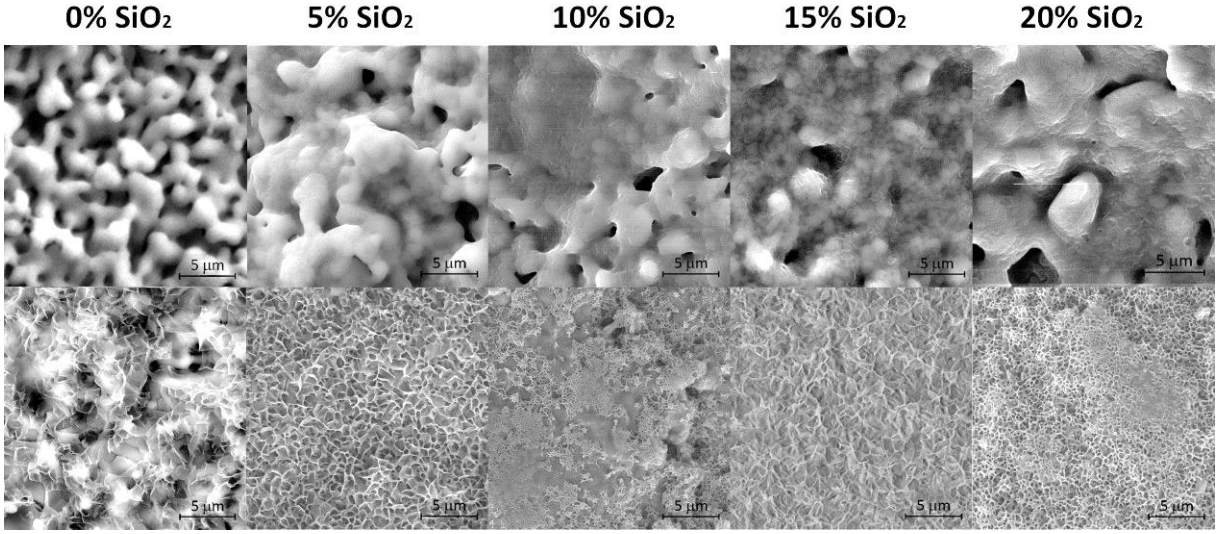

Fig. 19 Surfaces of HA-SiO_2 scaffolds before and after 3 day incubation in Eagle Medium.

Mechanical properties

Compressive strength of samples with initial pore size 60, 75 and 90 ppi was used for evaluation of the influence of silica content on mechanical properties of scaffolds.

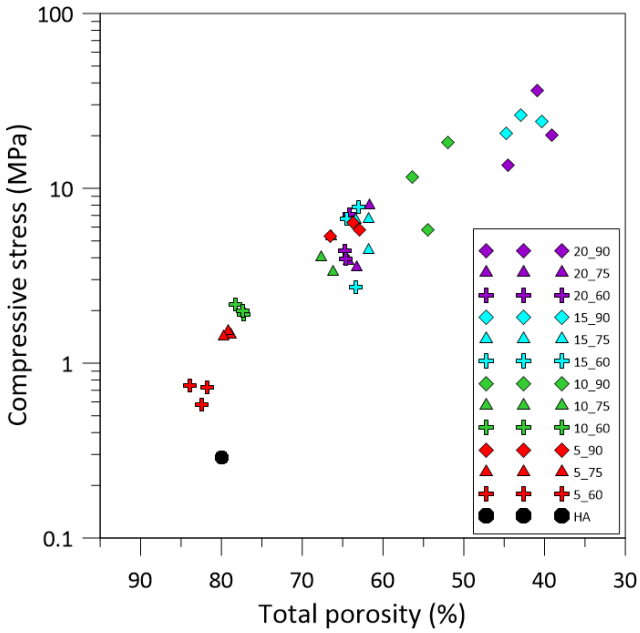

Fig. 20 Dependence of compressive strength on total porosity

Fig. 20 presents dependence of compressive strength on porosity of HA/SiO_2 scaffolds. Results indicated that strength exponentially increased with increasing density of scaffolds according to the Ryshkewitch-Duckworth [27, 28] equation.

$$\sigma = \sigma_0 \cdot e^{-cp}$$

Where the σ_0 is strength at zero porosity, c is constant (4–7 according to porosity) and p is porosity.

Silica had a positive influence on the strength, no matter if there were 5 or 20 percent of SiO_2 in HA/SiO_2 scaffolds. Moreover, it seemed that pore sizes also had negligible effect on final strength. One of the requirements imposed on the materials used in tissue engineering are properties similar to those of replaced tissues. In the case of cancellous bone, the compressive strength values were reported between 1.5 to 38 MPa [29], usually 2–20 MPa [30]. Strength-porosity dependence indicated that optimal strength for bone tissue replacement was achieved on the samples with lower porosity than 80%. Therefore compressive strength of the samples reinforced by silica are similar with those of bone and this type of composite material can be potentially used in bone tissue engineering.

4.5 Calcium phosphate scaffolds produced from CaP / PU composite foam

Thermal decomposition of CaP / PU scaffold

As was mentioned in Chapter 0, ceramic foams were obtained by burning out the polymer from the CaP / PU composites. To determine the temperature at which the thermal decomposition of polyurethanes is finished, the thermal analysis was carried out.

In general, the thermal degradation of polyurethanes in air atmosphere is a complex process involving oxidation of the initial polyol and isocyanate components, which is followed by the thermal decomposition that leads namely to the formation of amines, water and carbon dioxide [31, 32].

TA curves (performed on the sample HA100_2_105) are shown in Fig. 21. The total weight loss as a consequence of decomposition was 50 wt. %, which corresponded to the weight content of polyurethane in the input composition. The first endothermic drop on DTA curve below 100 °C was due to water evaporation. Increasing the temperature above 200 °C, the polyurethane started to decompose by a typical two stage process as is evident from the DTG and DTA curves. The weight loss, around 350 °C was caused by the degradation (oxidation) of hydroxyl and amino groups whereas the second stage, around 600 °C was mainly associated with the oxidation of the residual carbon.

Even though the decomposition of organic compounds was completely finished around 750 °C, the CaP / PU composites were heat treated at 800 °C/2 h to ensure the sufficient handling strength of presintered ceramic bodies.

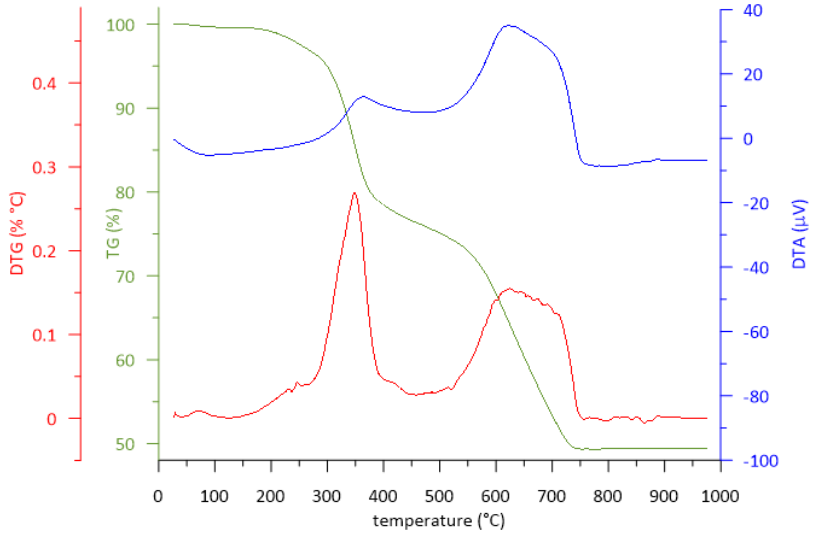

Fig. 21 TA analysis of polyurethane composite (HA100_2_105)

Foam characterisation - influence of chemical composition

Influence of the amount of added water, isocyanate index, ratio between calcium phosphate and polyurethane referred as CaP/PU ratio and sintering temperature on the final morphology was evaluated. Calculated values of total porosity are summarized in Table 3.

Table 3 Scaffold composition and total porosity at different temperatures

sample	Total porosity (%) calculated	Total porosity (%) 1050 °C/2 h	Total porosity (%) 1200 °C/2 h	Total porosity (%) 1350 °C/2 h
HA100_0_105	91.0 ± 1.8	87.0 ± 0.9	75.3	78.1
HA100_1_105	92.1 ± 0.7	86.9	83.6	83.6
HA100_2_105	92.3 ± 1.3	90.5	79.0	81.0
HA100_3_105	91.4 ± 0.7	85.2	79.5	82.2
HA100_4_105	92.2 ± 1.0	87.5	81.6	84.8
HA100_5_105	92.0 ± 0.5	87.4	81.3	80.4
HAu100_0_105	91.3 ± 0.6	83.0 ± 1.9	79.3	81.3
HAu100_2_105	93.9 ± 0.9	87.9	87.8	85.8
HAu100_4_105	90.7 ± 1.0	77.9	75.1	78.5
HA62_0_105	96.2 ± 0.1	90.9	88.4	88.2
HA56_1_105	97.0 ± 0.1	91.0	89.4	89.0

HA51_2_105	97.5 ± 0.6	91.7	91.3	90.7
HA47_3_105	97.3 ± 0.3	93.6	92.6	×
HA43_4_105	97.9 ± 0.2	×	×	×
HA40_5_105	98.0 ± 0.2	×	×	×
HA100_2_75	94.8 ± 0.4	90.7 ± 0.1	87.6	88.0
HA100_2_85	91.3 ± 0.5	85.3 ±1.8	79.0	76.9
HA100_2_95	93.0 ± 0.6	89.7 ±.6	81.8	82.7
HA100_2_115	93.0 ± 1.0	89.4	81.1	81.5
HA100_2_125	92.9 ± 0.8	86.7	84.5	84.1
HA40_2_105	97.8 ± 0.1	91.4	89.9	90.3
HA60_2_105	95.5 ± 0.1	91.7 ± 0.3	88.7	90.2
HA80_2_105	93.6 ± 0.4	86.8 ± 0.6	84.4	83.6
HA120_2_105	92.4	77.3	76.5	75.9
HA40_4_105	97.2 ± 0.2	×	×	×
HA60_4_105	96.4 ± 0.4	×	×	90.6
HA80_4_105	96.9 ± 0.7	90.0	87.5	88.7
HAu61_0_107	97.4 ± 0.5	91.2	89.7 ± 0.4	89.3
TCP74_0.5_95	96.8 ± 0.1	91.1	89.5 ± 0.3	76.1± 4.4

Effect of added water

Two sets of samples with an increasing amount of added water were evaluated (see Fig. 22). Pictures indicated that water addition (from 0 to 5 pphp) had a significant impact on the structure of the composites, mainly on pore size. During the processing water as blowing agent reacted with the NCO–functional groups of diisocyanate and formed unstable carbamic acid which immediately decomposed into an amine and carbon dioxide which caused generation of pores in the structure [33]. Reaction ran according to the following scheme:

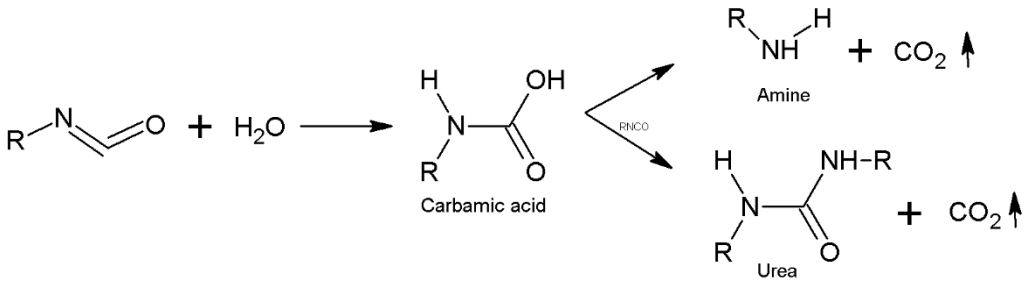

Fig. 22 CaP/PU foams having ha/pu ratio = 1 and I_{NCO} = 105 (water content increasing from 0 wt.% (left) to 5 wt% /(right) of polyol)

Theoretically, 1 mol of H_2O would create 22.4 dm^3 of CO_2. If all the created bubbles were stable and remained in the foam, the total volume (and apparent porosity) of the foam would rise with the increasing amount of water. However, this was not experimentally confirmed;

the results summarized in Fig. 23 indicated that apparent porosity was more or less independent on the water content. A slight increase of porosity of samples containing equal amount of powder as polyol was probably caused by different powder to polyurethane ratio, not by water.

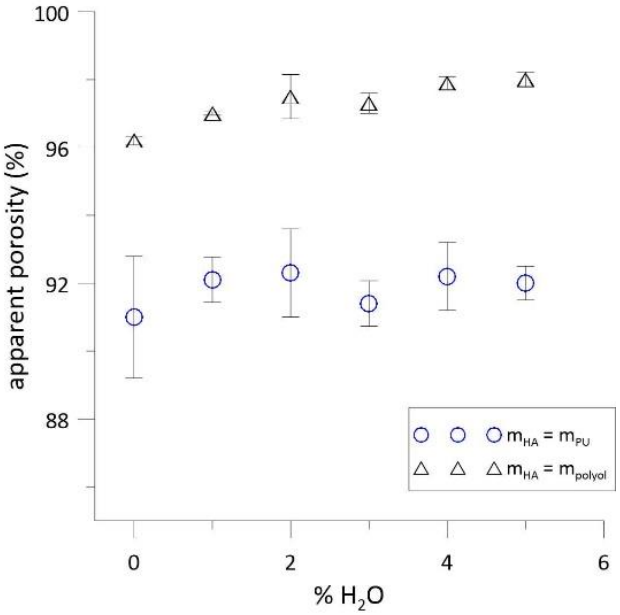

Fig. 23 Influence of water and powder content on porosity calculated from weight, dimensions and theoretical density of hydroxyapatite

Although the total volume of pores was almost the same, the additive water influenced individual pore sizes and their distribution (see Fig. 24 and Fig. 25). Pore sizes were determined by image analysis of polished cross sections cut 3 mm below the top of PU / HA foam, sintered at 1050 °C/2h. All pores having diameter larger than 5 μm were measured on the area 25 mm^2 per one sample. Results are summarized in Table 4. Since the pores were measured in 2D, the real (3D) diameters are larger [9]. Assuming that the pores are ideal spheres and according to the probability of cutting a sphere in different distances far from the largest diameter, the average pore diameters can be simply multiplied by a constant 1.254. This approach is not statistically completely right, detailed explanation of sphere unfolding and particle size distribution in 3D from 2D data can be found elsewhere [34-36].

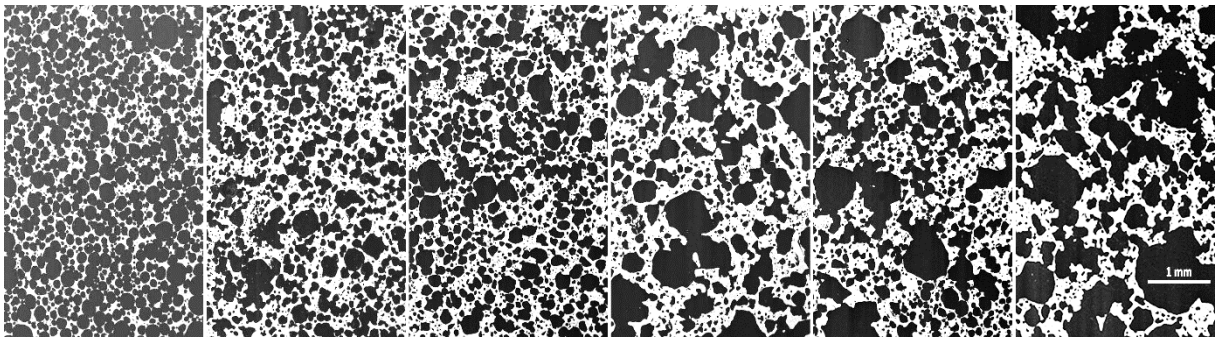

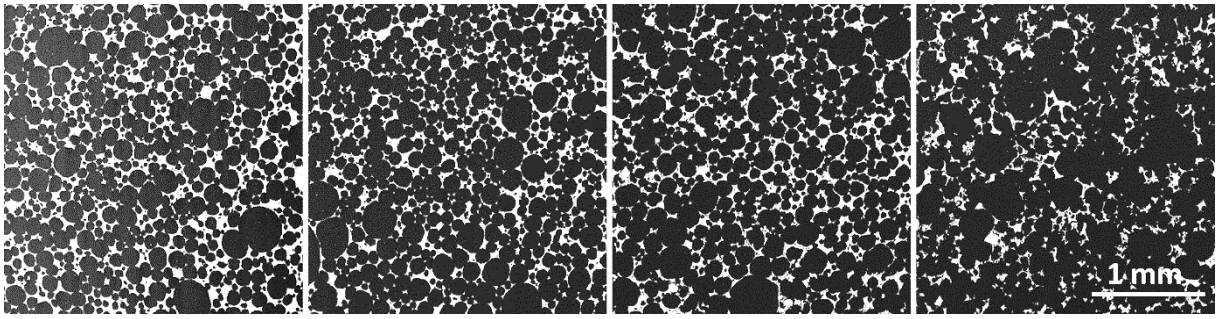

Fig. 24 Overview of cross sections of ceramic scaffolds sintered at 1050 °C: top row: $m_{HA} = m_{polyurethane}$, from 0 (left) to 5 pphp (right); bottom row: $m_{HA} = m_{polyol}$, from 0 (left) to 3 pphp (right)

As is obvious from Fig. 25, the pore size distribution (in 2D) was skewed right, the number of small pores was several times higher than the large ones. For differentiation of the influence of large and small pores which highly probably were not all slices of larger ones, an average size of 10% of the highest measured values was also calculated (see Table 4). It appeared that all of these large pores were interconnected and they formed the greater part of the surface area and they could be suitable for cell colonization.

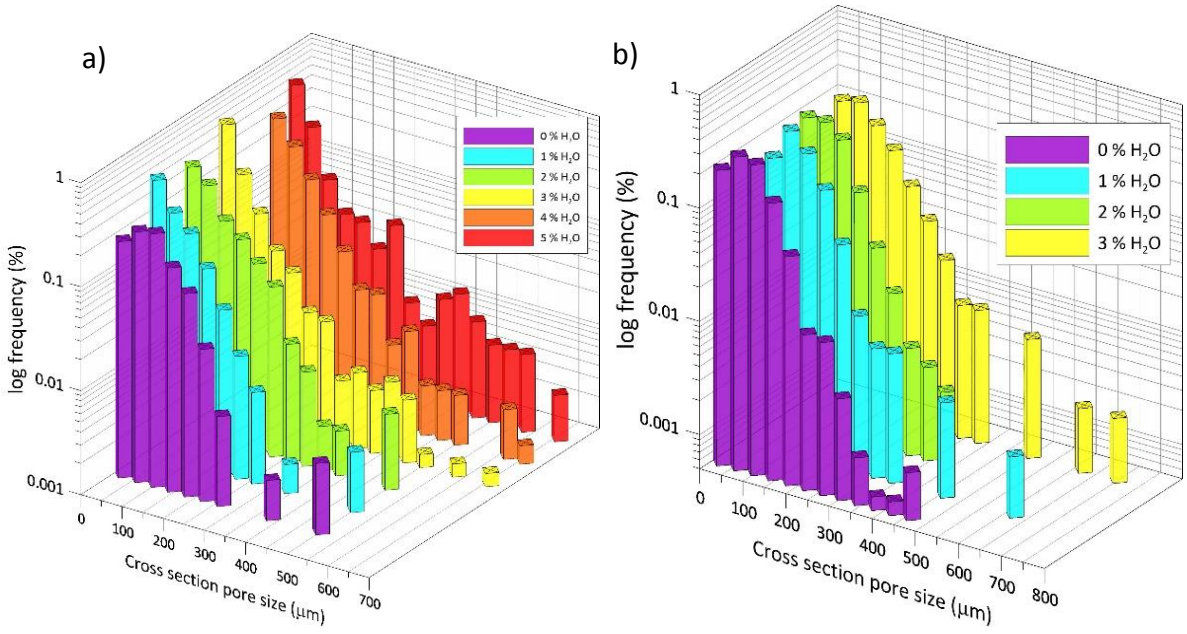

Fig. 25 Histograms of measured pore sizes: (a) $m_{HA} = m_{polyurethane}$; (b) $m_{HA} = m_{polyol}$

Table 4 Pore sizes estimated from cross section of scaffolds sintered at 1050 °C/2 h

HA/PU	1	1	1	1	1	1	0.62	0.56	0.51	0.47
H_2O (wt. % of polyol)	0	1	2	3	4	5	0	1	2	3
Porosity (image analysis)	78.8	61.0	64.8	59.7	60.6	67.2	81.7	84.7	85.9	88.4
Standard deviation (%)	0.5	2.3	2.6	1.2	2.9	2.9	0.6	0.7	0.3	1.3
Average pore size (µm)	94	65	79	65	86	93	86	125	109	124
Standard deviation (µm)	59	57	71	89	107	134	54	59	59	82
Avg pore size · 1.27 (µm)	120	83	100	83	110	118	110	159	139	158
10% largest pores (µm)	209	184	223	271	326	423	200	245	228	301
St. deviation 10% (µm)	59	61	79	144	157	169	57	77	47	99
Avg pores 10% · 1.27 (µm)	266	234	284	345	415	539	255	312	290	383

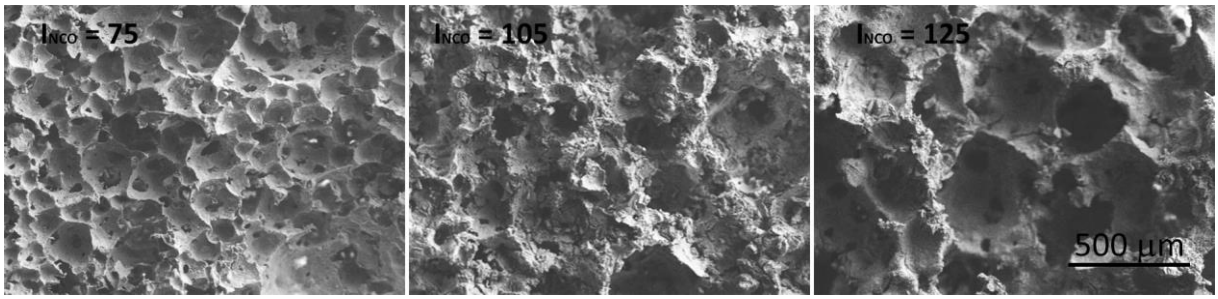

Fig. 26 Microstructrures of scaffolds with different isocyanate indexes (I_{NCO} = 75, 105, 125)

HA/PU = 100 %, 2 % H_2O, sintered at 1350 °C/2 h

Effect of sintering temperature

The microstructure was changed by the sintering temperature. PU/HA composite had very smooth surface as is evident from left quarter of Fig. 27 (PU+HA), the rough middle part of the same photo is a fracture area where the relief was caused by pulling out of ceramic particles. With an increasing temperature, the grains significantly coarsed and microporosity was reduced.

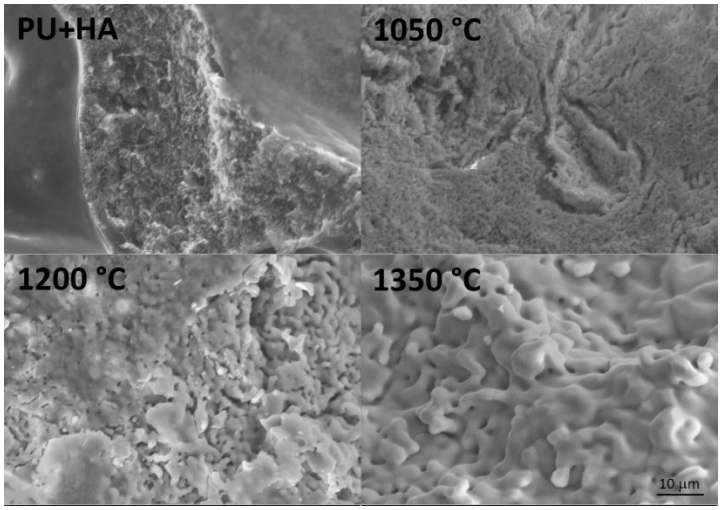

Fig. 27 Microstructures of HA100_2_105 scaffold sintered at different temperatures: (a) HA/PU composite before calcination; (b) scaffold sintered at 1050 °C; (c) 1200 °C; (d) 1350 °C (the magnification is the same for all 4 photos).

5 CONCLUSIONS

Open three-dimensional ceramic scaffolds with interconnected macropores were prepared by polymer replica technique or by polymerization in situ. Ceramic scaffolds were obtained in both cases after burning out the polyurethane and other binders from the structure. Regarding the replica technique, the morphology of scaffolds mimicked the morphology of commercial reticulated polyurethane templates. Cell size and its distribution was controlled by used template. The total porosity was tailored by viscosity of suspension and by number of applied layers.

The first studied system was based on alumina. Open-cell alumina foams were prepared by replica method from nanosized boehmite powder and fused microsized alumina. Highly porous reticulated alumina foams exhibited low compressive strength (< 0.25 MPa) because of high total porosity (> 95%), low microstructure density (~ 50%) and because of voids inside the struts generated during polyurethane burnout. The strength was at least doubled due to scaffold infiltration by nanosized boehmite, although the struts remained partially unfilled. The successful approach was strut filling by suspension composed of finer alumina particles having allowed about fourfold increase of strength. Mechanical properties were improved, however, material was biologically inert. To shift biological properties to bioactive behaviour, the foams were coated by hydroxyapatite suspension. All components, namely porous core, reinforcing phase (/layer) and bioactive coating, seemed to firmly adhere to each other. For application in bone tissue engineering it would be necessary to reduce pore sizes to maximally 500 μm and simultaneously improved the compressive strength, e.g. by decreasing total porosity below 85 %.

The second research area dealt with alumina toughened zirconia scaffolds. Macroporous scaffolds with interconnected pores of size ranging from 350 to 1200 μm were prepared by similar way as previously described foams. The difference was that yttria stabilized zirconia was used instead of fused alumina. Based on results of the mechanical testing, 5 wt. % content of alumina was chosen as optimum for further experiments. Scaffolds of various total porosity (57–98%) were fabricated by multiple coating process (up to 6 cycles). The bioactive behaviour of the composite was achieved by coating of calcium phosphates. Besides bioactivity and cytotoxicity tests, the cell colonization in 3D scaffold was evaluated. It was shown that MG-63 cells grew through the scaffold with 1000 μm large pores after three-day cultivation, the same amount of cells was found both adhered to the outer and inner struts of scaffold.

The main disadvantage of these two types of scaffolds was the bioinert core. The current trend of tissue engineering are resorbable materials that help bones to regenerate instead of formerly used permanent replacements, so the attention was focused on calcium phosphate scaffolds.

Calcium phosphate 3D interconnected scaffolds with different pore sizes were fabricated with and without silica addition. Pore dimensions ranging between 375 and 1150 μm were depended on the pore size of four templates which were replicated. The average window size between two interconnected pores was from 118 to 536 μm, ideal for cell penetration. Addition of silica (5– 20 wt. %) strongly influenced the phase transformation of hydroxyapatite to β–TCP and α–TCP, respectively. The ratio of α–TCP to β–TCP increased fivefold with increasing silica content. Lattice parameters indicated that TCP was substituted by silicate ions. However, almost all amorphous silica was transformed to the cristobalite crystalline

phase. Addition of cristobalite did not negatively influenced the biological properties. Testing in direct contact assay with MG63 cells showed that percentage of covered surface slightly increased with increasing silica content. After three days of cultivation, the surfaces were totally covered by newly formed apatite layer which indicates excellent bioactive behaviour. The cell viability increased with addition of silica; it seemed that silica supported cell adhesion. This trend was followed for the three pore sizes, with the maximum effect noted for the scaffolds using 90 ppi polymer pore size. The main enhancement was, nevertheless, observed on mechanical properties. The compressive strength of calcium phosphate scaffold bonded by polyvinylalcohol was 0.3 MPa at 80% porosity. The strength of silica reinforced calcium phosphates scaffolds exceeded 20 MPa.

From previous paragraph is obvious that preparation of calcium phosphate scaffolds by replica technique was from mechanical point of view less successful. For this reason a novel processing technique was developed to overcome the low strength caused by internal defects and hollow struts. Porous calcium phosphate scaffolds were successfully prepared by polymerization in situ using diisocyanate, polyol and water. Generation of carbon dioxide led to formation of large interconnected pores. Pores smaller than 5 μm were created by polymeric binder burnout during sintering. This small interconnected pores can be convenient for supply of nutrients and oxygen. The total porosity of scaffolds decreased from 99 to 76% as the powder content increased, leading to denser and thicker pore walls between interconnected pores. On the other hand, the total porosity was almost independent on amount of added water (up to 5 pphp, parts per hundred parts of polyol). However, water influenced pore size. Average pore size increased from 65 μm (1 pphp) to 93 μm (5 pphp). Sizes of 10 % of larges pores suitable for cell colonization were enlarged from 234 μm to 539 μm just due to water addition. Because the scaffolds are formed by in situ polymerization, the shape of scaffold can be easily controlled by the shape of mould. The porosity and pore size is tuneable just by powder / polyol / diisocanate / water ratio. On the basis of morphological observations, the calcium phosphate scaffolds could be promising adepts for synthetic bone grafts.

The aim of this thesis, to fabricate three-dimensional scaffolds that can be potentially used in bone tissue engineering, was achieved. Neither of the studied materials was cytotoxic and moreover all prepared composites behave bioactive in simulated body fluid. The most promising adept for application in bone tissue engineering seems to be composite material containing calcium phosphates reinforced by silica.

LITERATURE

[1] BOHNER, M. RESORBABLE BIOMATERIALS AS BONE GRAFT SUBSTITUTES, *MATERIALS TODAY,* 2010, VOL. 13, PP. 24.

[2] JONES, J. R.,BOCCACCINI, A. R. IN *CELLULAR CERAMICS*; WILEY-VCH VERLAG GMBH & CO. KGAA: 2006, P 547.

[3] LU, J., FLAUTRE, B., ANSELME, K., HARDOUIN, P., GALLUR, A., DESCAMPS, M.,THIERRY, B. ROLE OF INTERCONNECTIONS IN POROUS BIOCERAMICS ON BONE RECOLONIZATION IN VITRO AND IN VIVO, *JOURNAL OF MATERIALS SCIENCE: MATERIALS IN MEDICINE,* 1999, VOL. 10, PP. 111.

[4] LIU, Y., LIM, J.,TEOH, S. H. REVIEW: DEVELOPMENT OF CLINICALLY RELEVANT SCAFFOLDS FOR VASCULARISED BONE TISSUE ENGINEERING, *BIOTECHNOL ADV,* 2013, VOL. 31, PP. 688.

[5] HENCH, L. L. SOL-GEL MATERIALS FOR BIOCERAMIC APPLICATIONS, *CURRENT OPINION IN SOLID STATE AND MATERIALS SCIENCE,* 1997, VOL. 2, PP. 604.

[6] JONES, J. R.,HENCH, L. L. REGENERATION OF TRABECULAR BONE USING POROUS CERAMICS, *CURRENT OPINION IN SOLID STATE AND MATERIALS SCIENCE,* 2003, VOL. 7, PP. 301.

[7] HUTMACHER, D. W. SCAFFOLDS IN TISSUE ENGINEERING BONE AND CARTILAGE, *BIOMATERIALS,* 2000, VOL. 21, PP. 2529.

[8] STAFF, B. S. I. *ADVANCED TECHNICAL CERAMICS. MONOLITHIC CERAMICS. GENERAL AND TEXTURAL PROPERTIES. DETERMINATION OF DENSITY AND POROSITY*; B S I STANDARDS, 1993.

[9] LOCK, P. A., JING, X. D., ZIMMERMAN, R. W.,SCHLUETER, E. M. PREDICTING THE PERMEABILITY OF SANDSTONE FROM IMAGE ANALYSIS OF PORE STRUCTURE, *JOURNAL OF APPLIED PHYSICS,* 2002, VOL. 92, PP. 6311.

[10] KOKUBO, T.,TAKADAMA, H. HOW USEFUL IS SBF IN PREDICTING IN VIVO BONE BIOACTIVITY?, *BIOMATERIALS,* 2006, VOL. 27, PP. 2907.

[11] FRANCO, R., NGUYEN, T.,LEE, B.-T. PREPARATION AND CHARACTERIZATION OF ELECTROSPUN PCL/PLGA MEMBRANES AND CHITOSAN/GELATIN HYDROGELS FOR SKIN BIOENGINEERING APPLICATIONS, *JOURNAL OF MATERIALS SCIENCE: MATERIALS IN MEDICINE,* 2011, VOL. 22, PP. 2207.

[12] GOLUNOVA, A., JAROŠ, J., JURTÍKOVÁ, V., KOTELNIKOV, I., KOTEK, J., HLÍDKOVÁ, H., STREIT, L., HAMPL, A., RYPÁČEK, F.,PROKS, V. N-(2-HYDROXYPROPYL) METHACRYLAMIDE BASED CRYOGELS–SYNTHESIS AND BIOMIMETIC MODIFICATION FOR STEM CELL APPLICATIONS, *PHYSIOLOGICAL RESEARCH/ACADEMIA SCIENTIARUM BOHEMOSLOVACA,* 2015, VOL. 64, PP. S19.

[13] GREGOROVÁ, E., PABST, W., ŽIVCOVÁ, Z., SEDLÁŘOVÁ, I.,HOLÍKOVÁ, S. POROUS ALUMINA CERAMICS PREPARED WITH WHEAT FLOUR, *JOURNAL OF THE EUROPEAN CERAMIC SOCIETY,* 2010, VOL. 30, PP. 2871.

[14] VOGT, U. F., GORBAR, M., DIMOPOULOS-EGGENSCHWILER, P., BROENSTRUP, A., WAGNER, G.,COLOMBO, P. IMPROVING THE PROPERTIES OF CERAMIC FOAMS BY A VACUUM INFILTRATION PROCESS, *JOURNAL OF THE EUROPEAN CERAMIC SOCIETY,* 2010, VOL. 30, PP. 3005.

[15] STUDART, A. R., GONZENBACH, U. T., TERVOORT, E.,GAUCKLER, L. J. PROCESSING ROUTES TO MACROPOROUS CERAMICS: A REVIEW, *JOURNAL OF THE AMERICAN CERAMIC SOCIETY,* 2006, VOL. 89, PP. 1771.

[16] ZHAO, Y., JIANG, L., LIAO, Y., WANG, C., LU, J., ZHANG, J.,LI, W. LOW TEMPERATURE DEGRADATION OF ALUMINA-TOUGHENED ZIRCONIA IN ARTIFICIAL SALIVA, *J. WUHAN UNIV. TECHNOL.-MAT. SCI. EDIT.,* 2013, VOL. 28, PP. 844.
[17] KELLER, T. S. PREDICTING THE COMPRESSIVE MECHANICAL BEHAVIOR OF BONE, *JOURNAL OF BIOMECHANICS,* 1994, VOL. 27, PP. 1159.
[18] NIKOM, J., CHAROONPATRAPONG-PANYAYONG, K., KEDJARUNE-LEGGAT, U., STEVENS, R., KOSACHAN, N.,JAROENWORALUCK, A. 3D INTERCONNECTED POROUS HA SCAFFOLDS WITH SIO2 ADDITIONS: EFFECT OF SIO2 CONTENT AND MACROPORE SIZE ON THE VIABILITY OF HUMAN OSTEOBLAST CELLS, *J BIOMED MATER RES A,* 2013, VOL. 101, PP. 2295.
[19] CIHLÁŘ, J., BUCHAL, A.,TRUNEC, M. KINETICS OF THERMAL DECOMPOSITION OF HYDROXYAPATITE BIOCERAMICS, *JOURNAL OF MATERIALS SCIENCE,* 1999, VOL. 34, PP. 6121.
[20] LIAO, C.-J., LIN, F.-H., CHEN, K.-S.,SUN, J.-S. THERMAL DECOMPOSITION AND RECONSTITUTION OF HYDROXYAPATITE IN AIR ATMOSPHERE, *BIOMATERIALS,* 1999, VOL. 20, PP. 1807.
[21] PIETAK, A. M., REID, J. W., STOTT, M. J.,SAYER, M. SILICON SUBSTITUTION IN THE CALCIUM PHOSPHATE BIOCERAMICS, *BIOMATERIALS,* 2007, VOL. 28, PP. 4023.
[22] REID, J. W., PIETAK, A., SAYER, M., DUNFIELD, D.,SMITH, T. J. N. PHASE FORMATION AND EVOLUTION IN THE SILICON SUBSTITUTED TRICALCIUM PHOSPHATE/APATITE SYSTEM, *BIOMATERIALS,* 2005, VOL. 26, PP. 2887.
[23] SAYER, M., STRATILATOV, A., REID, J., CALDERIN, L., STOTT, M., YIN, X., MACKENZIE, M., SMITH, T., HENDRY, J.,LANGSTAFF, S. STRUCTURE AND COMPOSITION OF SILICON-STABILIZED TRICALCIUM PHOSPHATE, *BIOMATERIALS,* 2003, VOL. 24, PP. 369.
[24] SAYER, M., STRATILATOV, A. D., REID, J., CALDERIN, L., STOTT, M. J., YIN, X., MACKENZIE, M., SMITH, T. J. N., HENDRY, J. A.,LANGSTAFF, S. D. STRUCTURE AND COMPOSITION OF SILICON-STABILIZED TRICALCIUM PHOSPHATE, *BIOMATERIALS,* 2003, VOL. 24, PP. 369.
[25] LANGSTAFF, S., SAYER, M., SMITH, T., PUGH, S., HESP, S.,THOMPSON, W. RESORBABLE BIOCERAMICS BASED ON STABILIZED CALCIUM PHOSPHATES. PART I: RATIONAL DESIGN, SAMPLE PREPARATION AND MATERIAL CHARACTERIZATION, *BIOMATERIALS,* 1999, VOL. 20, PP. 1727.
[26] REID, J. W., TUCK, L., SAYER, M., FARGO, K.,HENDRY, J. A. SYNTHESIS AND CHARACTERIZATION OF SINGLE-PHASE SILICON-SUBSTITUTED A-TRICALCIUM PHOSPHATE, *BIOMATERIALS,* 2006, VOL. 27, PP. 2916.
[27] DUCKWORTH, W. DISCUSSION OF RYSHKEWITCH PAPER BY WINSTON DUCKWORTH*, *JOURNAL OF THE AMERICAN CERAMIC SOCIETY,* 1953, VOL. 36, PP. 68.
[28] RYSHKEWITCH, E. COMPRESSION STRENGTH OF POROUS SINTERED ALUMINA AND ZIRCONIA, *JOURNAL OF THE AMERICAN CERAMIC SOCIETY,* 1953, VOL. 36, PP. 65.
[29] PACE, A., VALENZA, A.,VITALE, G. MECHANICAL CHARACTERIZATION OF HUMAN CANCELLOUS BONE TISSUE BY STATIC COMPRESSION TESTS, *I MATERIALI BIOCOMPATIBILI PER LA MEDICINA/BIOMATERIALS FOR MEDICINE: ATTI DEL CONVEGNO NAZIONALE DELLA SOCIETÀ ITALIANA BIOMATERIALI. PALERMO, 2-4 LUGLIO 2014,* 2014, VOL., PP. 15.
[30] OLSZTA, M. J., CHENG, X., JEE, S. S., KUMAR, R., KIM, Y.-Y., KAUFMAN, M. J., DOUGLAS, E. P.,GOWER, L. B. BONE STRUCTURE AND FORMATION: A NEW PERSPECTIVE, *MATERIALS SCIENCE AND ENGINEERING: R: REPORTS,* 2007, VOL. 58, PP. 77.

[31] SOMANI, K. P., KANSARA, S. S., PATEL, N. K.,RAKSHIT, A. K. CASTOR OIL BASED POLYURETHANE ADHESIVES FOR WOOD-TO-WOOD BONDING, *INTERNATIONAL JOURNAL OF ADHESION AND ADHESIVES,* 2003, VOL. 23, PP. 269.
[32] PISZCZYK, Ł., STRANKOWSKI, M., DANOWSKA, M., HEJNA, A.,HAPONIUK, J. T. RIGID POLYURETHANE FOAMS FROM A POLYGLYCEROL-BASED POLYOL, *EUROPEAN POLYMER JOURNAL,* 2014, VOL. 57, PP. 143.
[33] SHARMIN, E.,ZAFAR, F. POLYURETHANE: AN INTRODUCTION, 2012, VOL., PP.
[34] PAYTON, E. J. REVISITING SPHERE UNFOLDING RELATIONSHIPS FOR THE STEREOLOGICAL ANALYSIS OF SEGMENTED DIGITAL MICROSTRUCTURE IMAGES, *JOURNAL OF MINERALS AND MATERIALS CHARACTERIZATION AND ENGINEERING,* 2012, VOL. VOL.11NO.03, PP. 22.
[36]TAKAHASHI, J.,SUITO, H. EVALUATION OF THE ACCURACY OF THE THREE-DIMENSIONAL SIZE DISTRIBUTION ESTIMATED FROM THE SCHWARTZ-SALTYKOV METHOD, *METALL AND MAT TRANS A,* 2003, VOL. 34, PP. 171.

Europass Curriculum Vitae

Personal information

First name(s) / Surname(s)	**Lenka NOVOTNÁ**
Address(es)	Helceletova 5, Brno, 602 00
Telephone(s)	(+420) 541 14 33 40
E-mail	lenka.novotna@ceitec.vutbr.cz
Nationality	Czech
Date of birth	03.06.1985
Gender	Female

Education and training

Dates	July 2010 onwards
Principal subjects/occupational skills covered	Ph.D. student, specialized in material engineering
Name and type of organisation providing education and training	Brno University of Technology, Faculty of Mechanical Engineering
Dates	September 2005 – June 2010
Principal subjects/occupational skills covered	masters degree, title achieved: Ing. material engineering diploma work: Propagation of inclined cracks to the interface of ceramic laminates
Name and type of organisation providing education and training	Brno University of Technology, Faculty of Mechanical Engineering

Personal skills and competences

Mother tongue(s): **Czech**

Other language(s)

Self-assessment	Understanding				Speaking				Writing	
European level (*)	Listening		Reading		Spoken interaction		Spoken production			
English	C1	Advanced user	C1	Advanced user	C1	Advanced user	C1	Advanced user	C1	Advanced user
Italian	B1	Independent user	B1	Independent user	B1	Independent user	B1	Independent user	B1	Independent user

(*) Common European Framework of Reference for Languages

Social skills and competences	good communication ability team work
Technical skills and competences	SEM analysis, image analysis Preparation of ceramographic specimens
Computer skills and competences	excellent knowledge on Microsoft Office applications

ABSTRACT

The aim of this thesis was to prepare three-dimensional scaffolds that can be potentially used for the reconstruction and regeneration of damaged bone tissues. Two techniques were used to create the porous ceramic scaffolds – polymer replica technique and polymerization in situ. A variety of bioceramic materials were studied, mainly alumina, zirconia and calcium phosphates. The effect of processing parameters, such as composition of suspensions, as well as the effect of heat treatment on structure and final properties of the prepared scaffolds were evaluated. Morphology of the sintered scaffolds was characterised by scanning electron microscopy; in particular pore size, pores interconnection, total porosity and density were described. Phase composition, compressive strength and biological properties such as bioactivity and cytotoxicity were also discussed.

The dissertation is divided into several sections. The literature review briefly summarizes the structure and properties of bones, the requirements for scaffolds, advantages and disadvantages of currently used materials and methods of ceramic foam preparation. The first part of experiments dealt with scaffolds prepared by polymer replica technique. All fabricated foams had interconnected pores with size in the range of 300 to 2000 μm, total porosity was 50–99%. The compressive strength of calcium phosphate foams prepared by replica technique reached about 0.3 MPa (at 80 % porosity). Reinforcement of the scaffolds was reached by using bio-inert cores or by incorporation of silica into the composite structure. The strength of calcium phosphate/silica scaffold increased above 20 MPa. The last section of experimental part discusses in situ blown calcium phosphate scaffolds, created by using the formation process of polyurethane foam with diisocyanate and polyol components. The sintered scaffolds had mainly interconnected macroporous structure with pore size ranging 80 to 550 μm. The total porosity was about 76 to 99 %. The advantage of this method compared to the polymer replica technique was that the struts were completely filled.

None of the studied materials was cytotoxic and moreover all studied foams exhibited bioactive behaviour. The most promising adept for application in bone tissue engineering seems to be composite material containing calcium phosphates reinforced by silica.

ABSTRAKT

Cílem disertační práce bylo připravit trojrozměrné biokeramické podpůrné systémy („skafoldy“), které by v budoucnu mohly pomoci při rekonstrukci a regeneraci poškozených kostních tkání. Porézní keramické pěny byly připraveny dvěma způsoby – replikační technikou a polymerizací in situ. Co se složení týče, byly studovány keramické materiály zejména na bázi oxidu hlinitého, zirkoničitého a kalcium fosfátů. Byl studován jednak vliv procesních parametrů jako je složení suspenzí a jejich viskozit, dále pak vliv tepelného zpracování na strukturu a výsledné vlastnosti připravených materiálů. U slinutých pěn byla pomocí rastrovací elektronové mikroskopie hodnocena zejména morfologie – velikost pórů, jejich propojenost a celková porozita, charakterizace mikrostruktury nebyla opomenuta. Dále bylo stanoveno fázové složení a pevnost v tlaku. Z biologických vlastností byla testována a diskutována bioaktivita a cytotoxicita materiálů.

Disertační práce je členěna do několika částí. V literární rešerši je popsána stavba a vlastnosti kosti, požadavky kladené na kostní náhrady, výhody a nevýhody současně používaných materiálů a způsoby přípravy keramických pěn. Následuje experimentální část, kde byly

nejprve studovány pěny připravené replikační technikou. Všechny takto vyrobené pěny měly propojené póry o velikostech 300 až 2000 μm, celková porozita se pohybovala v rozmezí 50 – 99 %. Pevnost pěn na bázi kalcium fosfátů – 0,3 MPa (při celkové porozitě 80%) byla nedostatečná pro kostní náhrady, kde je požadována pevnost větší než 2 MPa. Kalcium fosfátové keramiky byly tedy zpevněny buďto inertním jádrem na bázi oxidu hlinitého nebo ATZ (oxidem zirkoničitým zhouževnatělým oxidem hlinitým). Dále byl přípraven částicový kompozit, ve kterým byl hydroxyapatit pojený oxidem křemičitým. Pevnost pěn se podařilo zvýšit až na více než 20 MPa. V poslední kapitole experimentální části byly studovány keramické pěny pěněné in situ, kde byly póry vytvářeny oxidem uhličitým unikajícím během reakce mezi diisokyanátem a polyalkoholem. Po vypálení polymerního pojiva měly pěny propojené póry o průměrné velikosti 80 až 550 μm. Celková porozita se pohybovala v rozmezí 76 – 99%. Výhodou oproti replikační technice byly plné trámečky bez velké středové dutiny vznikající vypálením polymerní předlohy.

Žádný ze studovaných materiálů nebyl pro buňky toxický, navíc všechny studované pěny vykazovaly bioaktivní chování. Z hlediska kostního tkáňového inženýrství se jako nejslibnější jeví kompozitní materiál zpevněný oxidem křemičitým.